IEEE Photonics Journal
An IEEE Photonics Society Publication

Open Access

Tunable Large Dispersion in Hybrid Modes of Lithium Niobate-on-Insulator Multimode Waveguides

Volume 11, Number 3, June 2019

Archana Kaushalram, *Student Member, IEEE*
Shafeek Abdul Samad
Gopalkrishna Hegde
Srinivas Talabattula, *Senior Member, IEEE*

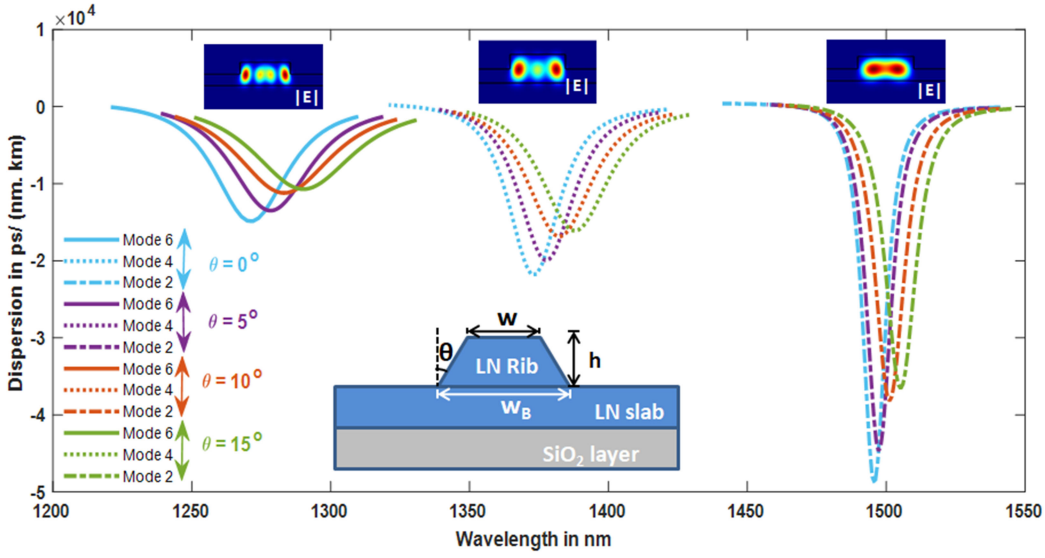

DOI: 10.1109/JPHOT.2019.2918759
1943-0655 © 2019 IEEE

Tunable Large Dispersion in Hybrid Modes of Lithium Niobate-on-Insulator Multimode Waveguides

Archana Kaushalram,[1] ***Student Member, IEEE***,
Shafeek Abdul Samad,[1] **Gopalkrishna Hegde**,[2]
and Srinivas Talabattula,[1] ***Senior Member, IEEE***

[1]Department of Electrical Communication Engineering, Indian Institute of Science, Bengaluru 560012, India
[2]Centre for BioSystems and Engineering, Indian Institute of Science, Bengaluru 560012, India

DOI:10.1109/JPHOT.2019.2918759

Manuscript received March 26, 2019; revised May 13, 2019; accepted May 20, 2019. Date of publication May 23, 2019; date of current version June 6, 2019. Corresponding author: Archana Kaushalram (e-mail: archana@iisc.ac.in).

Abstract: We report a large group velocity dispersion of hybrid modes in a LiNbO3-on-insulator multimode rib waveguide. A peak dispersion of $\pm$49000 ps/(nm.km) is obtained in the mode hybridization region between TE_{00} and TM_{10} modes with a full width at half maximum of 10 nm. Dispersion for hybrid modes is tunable around $\pm$15000 ps/(nm.km), $\pm$22000 ps/(nm.km), and $\pm$49000 ps/(nm.km) occurring at wavelengths of 1272, 1372, and 1496 nm, respectively, in the telecommunication band. In the wavelength range from 1530 to 1600 nm, the proposed rib waveguide is free of hybrid modes. In this region, the waveguide exhibits a flat dispersion profile for all eight guided modes with a maximum $<$1000 ps/(nm.km).

Index Terms: Multimode waveguide, lithium niobate-on-insulator, dispersion, hybrid modes.

1. Introduction

Lithium niobate (LN) is a popular integrated photonics platform with a broad transparency range of 350 nm to 5200 nm, strong electro-optic, acousto-optic, and thermo-optic effects [1], [2]. These properties make LN an excellent choice for passive as well as active and non-linear devices. LN also has high intrinsic birefringence that has been used to design modal birefringence-free waveguides [3]. Traditional waveguides in lithium niobate used titanium diffusion or proton exchange to create a refractive index contrast of $\sim$0.01 between the core and the clad [4]. These resulted in large waveguide cross sections with mode diameter spanning up to 8 μm. However, the advent of recent thin film lithium niobate on insulator with either silicon or LN as the substrate has led to an index contrast of $\sim$0.7. This has led to ultra-compact and strong guiding LN photonic wires, being realized on the single-crystal LN films. The large index contrast also enhances the performance of active optical components, such as wavelength conversion devices, ring resonators [5], and waveguide lasers [6]. Such photonic wires also enable high integration density of photonic devices on chip. Recent advances in fabrication techniques has resulted in lithium niobate on insulator (LNOI) waveguides with a propagation loss as low as 0.027 dB/cm [7].

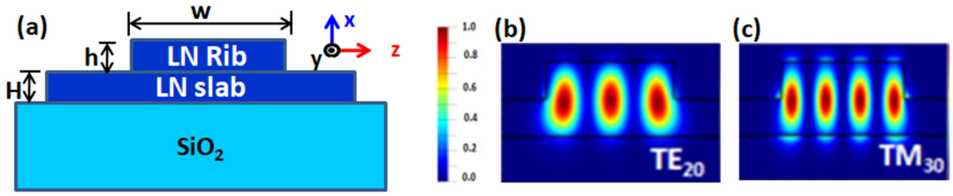

Fig. 1. (a) Cross-section of LN (X-cut) rib waveguide (b) Mode profile of TE_{20} and (c) TM_{30}.

Multimode LN waveguides are being investigated for applications like optical interconnects in mode division multiplexing (MDM) that increase the channel capacity [8]. MDM components need waveguides with only quasi transverse electric (*qTE*) and quasi transverse magnetic (*qTM*) modes without any hybrid modes. However, the phenomenon of mode hybridization is common in waveguides with horizontal or/and vertical index asymmetry [9]. Hybrid modes which are neither *qTE* nor *qTM* exist if effective indices of different polarized modes with the same symmetry have similar values [10]. Such modes result in data exchange between channels on the two coupled modes, leading to crosstalk [11].

Multimode waveguides with low group velocity dispersion (GVD) are desirable in optical communications to preserve the shape of ultra-short pulses and increase the data rate. However, components with large dispersion are crucial for applications including pulse compression, tunable delays, optical correlation [12], frequency combs, ultra-fast waveguide lasers, bright soliton formation and supercontinuum generation [13]. Various approaches have been proposed in literature to achieve large dispersion using micro ring resonators [14], integrated Bragg gratings [15], photonic crystal waveguides and slot waveguides [16]. One of the methods is to enhance interaction between modes in a coupled strip-slot waveguide [17]. Dispersion increases by orders of magnitude at a wavelength where the super modes are resonant-coupled, compared to qTE and qTM modes [12].

In this paper, we report a huge *GVD* (anomalous and normal) of hybrid modes in a multimode rib waveguide on LNOI platform. The proposed waveguide has large dispersion at three mode hybridization regions when the wavelength (λ) is varied from 1200 nm to 1500 nm in the telecommunication band. Each hybrid mode has a different dispersion, facilitating tunable dispersion with change in wavelength. Also, this waveguide has much lower dispersion ($<$1000 ps/nm.km) when it is operated in the wavelength range of 1530 nm to 1600 nm, supporting only *qTE* and *qTM* modes. Dispersion in this wavelength range is comparable to that of single-mode silicon nitride waveguides [18] and much lower than that in silicon counterparts [19].

This paper is organized into three more sections, second section describes the methodology and simulation parameters, third section has the simulation results, and fourth section concludes the paper.

2. Methodology

The cross section of rib waveguide analyzed in this work is shown in Fig. 1(a) with a width (w) of 3.75 μm and a height (h) of 0.4 μm, with the slab height (H) fixed at 0.4 μm. The underlying clad is silicon dioxide of thickness 2 μm, which can be grown on a silicon or LN substrate. Numerical analysis is carried out using a full-vectorial finite-difference Eigen mode solver [20]. The wavelength dependent refractive index of LN is modeled using Sellmeier equation from literature [21]. Mode profiles of TE_{20} and TM_{30} higher order guided modes are shown in Fig. 1(b) and (c). The variation of effective index (n_{eff}) of guided modes with the rib width (w) at a wavelength of 1550 nm is shown in Fig. 2. It is observed that there are no anti-crossings, indicating that there are no hybrid modes at this wavelength.

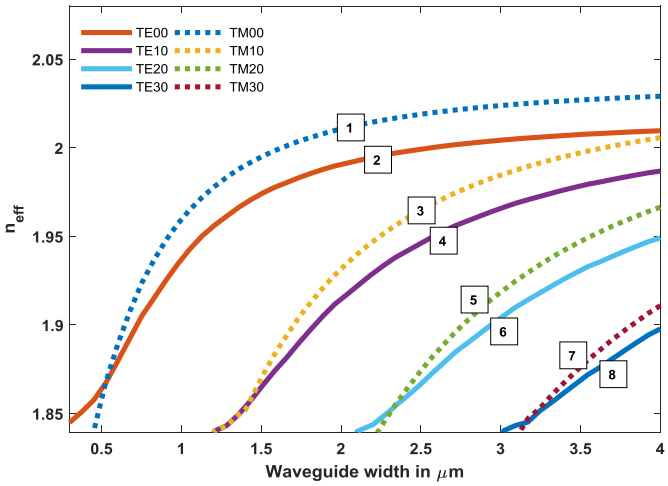

Fig. 2. Variation of effective indices (n_{eff}) of guided *qTE* and *qTM* modes with the rib width (w).

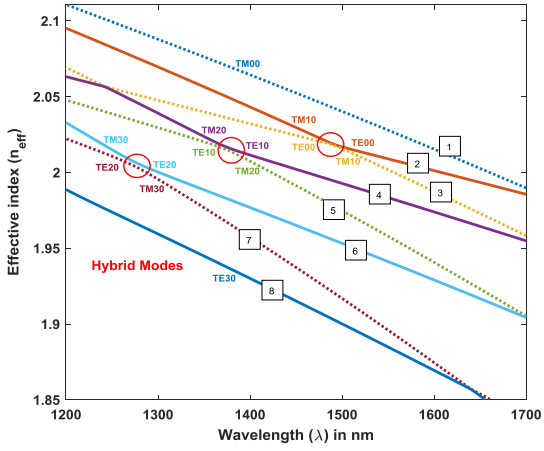

Fig. 3. Variation of effective indices of guided *qTE* and *qTM* modes with wavelength.

3. Results

The effective indices and mode hybridizations are strong functions of wavelength as inferred from Fig. 3. Three hybridization regions (anti-crossings) are marked in red circles, first one between TE_{20} and TM_{30} at λ of 1272 nm; second one between TE_{10} and TM_{20} at λ of 1372 nm; third one between TE_{00} and TM_{10} at λ of 1496 nm. The corresponding differences between effective indices (Δn_{eff}) of the coupled modes are 0.0029, 0.0018, and 0.0008. Normalized electric field intensity distributions along with the dominant and non-dominant electric field components of the two hybrid modes at a wavelength of 1372 nm are shown in Fig. 4.

Mode hybridization is quantified by TE polarization fraction (γ_{TE}), which indicates fraction of power from the dominant field component of a mode.

$$\gamma_{TE} = \frac{\int |E_z|^2 dx dz}{\int \left(|E_z|^2 + |E_x|^2\right) dx dz} \tag{1}$$

γ_{TE} is 1 for *qTE* modes and 0 for *qTM* modes. It is ~0.5 when hybridization is maximum. γ_{TE} as a function of waveguide rib width at a wavelength of 1550 nm in Fig. 5(a) shows absolutely no hybrid modes. γ_{TE} as a function of wavelength for a fixed waveguide cross section (3.75 μm $\times$ 0.4 μm) is

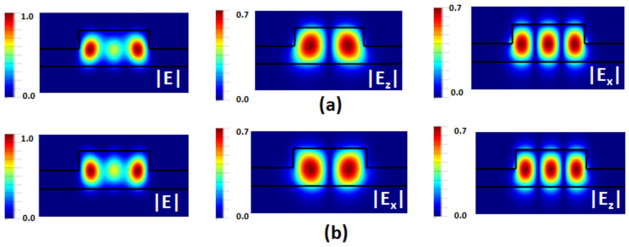

Fig. 4. Normalized electric field intensity |E|, dominant field component and non-dominant field components of (a) Mode 4 and (b) Mode 5.

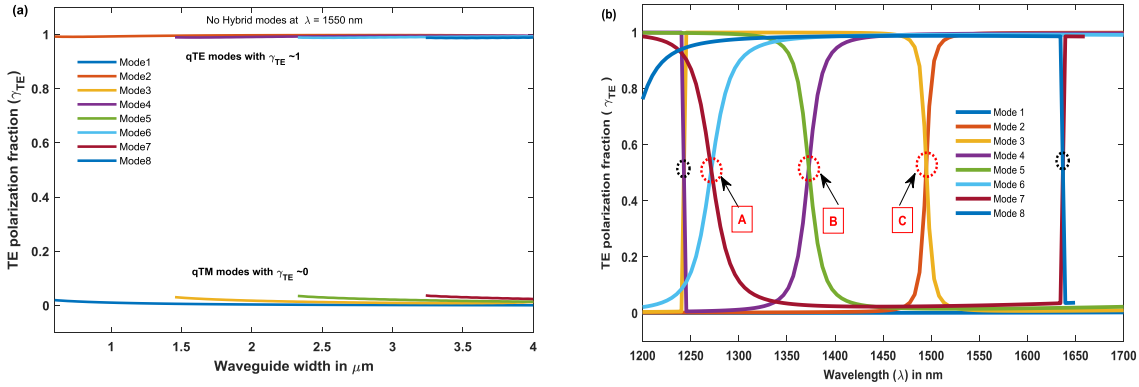

Fig. 5. Variation of TE polarization fraction with (a) rib width at a wavelength of 1550 nm (b) wavelength (λ) with a rib width of 3.75 μm and height of 0.4 μm.

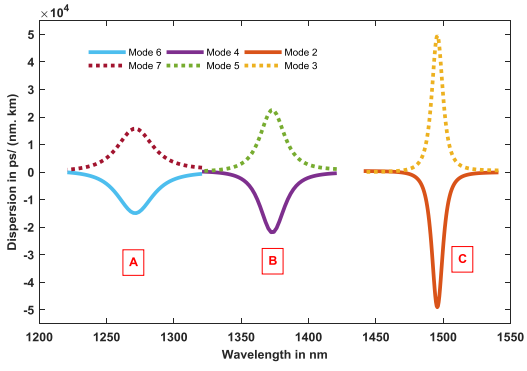

Fig. 6. Dispersion profile in the regions of mode hybridization between Modes 6 and 7, modes 4 and 5, modes 2 and 3.

shown in Fig. 5(b). This design has three hybridization regions marked in red circles (A, B, and C) with $\gamma_{TE} \sim 0.5$. Nearly vertical transitions marked with black circles indicate just the change in the mode order. There is no hybridization and no mode coupling in these regions.

Dispersion values at the hybridization regions are shown in Fig. 6. While the nearly *qTE* mode in the hybrid region has a large negative dispersion, corresponding *qTM* mode exhibits an almost equal positive dispersion. Such large dispersion results from strong interaction between the coupling modes. Magnitude of peak dispersions obtained are ~15000, 22000, and 49000 ps/(nm.km) for the hybrid regions, A, B, and C respectively as shown in Fig. 6. The corresponding full widths at

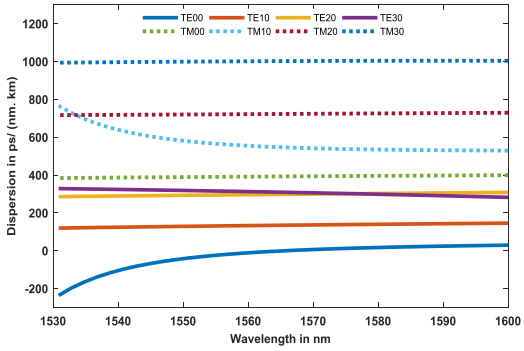

Fig. 7. Dispersion profile for qTE and qTM modes.

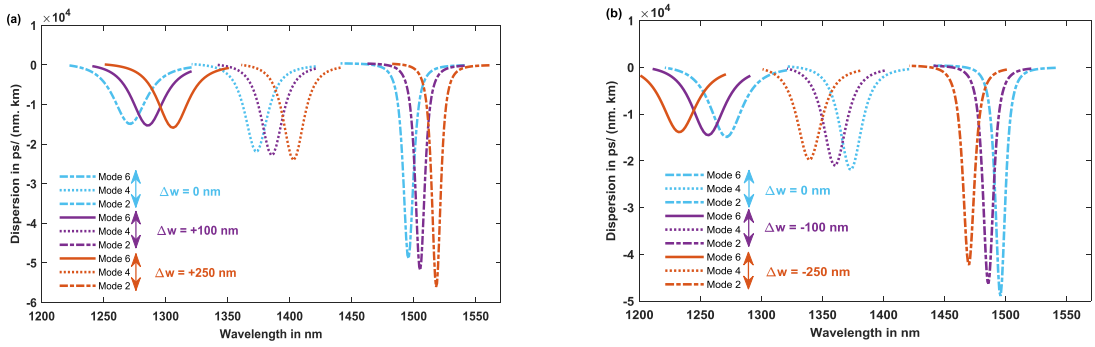

Fig. 8. Effect of (a) increase in rib width (b) decrease in rib width on dispersion profile of hybrid modes.

half maxima (FWHM) of dispersion are found to be 30 nm, 21 nm, and 10 nm. It is observed that smaller the Δn_{eff} of the coupling modes, higher is the dispersion and narrower the bandwidth.

Dispersion in the vicinity of hybrid modes is orders of magnitude larger than that of *qTE* and *qTM* modes. This can be observed by comparing Fig. 6 with Fig. 7, which illustrates *GVD* for guided *qTE* and *qTM* modes for the narrow range of 1530 to 1600 nm without any hybrids. All modes have a dispersion with magnitude $<$1000 ps/(nm.km).

Large anomalous and normal dispersion is reported on silicon [12], which uses a vertical stack of a strip and a slot. But the current work focuses on LN and, large dispersion is obtained with mode hybridization between modes of a simple rib waveguide. The relatively lower dispersion values in LN waveguides compared to silicon on insulator (SOI) can be attributed to the lower index contrast and larger cross section.

Further, we extend our analysis to include fabrication tolerances in rib width and height. Fabrication errors affect mode hybridization regions, both the magnitude of dispersion as well as the wavelengths of their occurrence. Deviation from the designed rib width '*w*' and rib height '*h*' are represented as Δw and Δh respectively. Dispersion of nearly qTE hybrid modes at different Δw are shown in Fig. 8. It can be noted that dispersion peaks red shift with the increase in rib width, and the corresponding peak values increase [see Fig. 8(a)]. Peak value of dispersion for mode 2 shows an increase of 15% when the rib width increases by 250 nm. However, no significant change was observed in FWHM bandwidth. With the reduction in rib width, dispersion peaks blue shift, and the corresponding dispersion values also decrease [see Fig. 8(b)]. Effects of rib height variation on dispersion profile are illustrated in Fig. 9. The resonant wavelengths for the hybrid modes do not drift significantly with the changes in rib height (etch depth). However, the magnitude of peak dispersion increased with the increase in rib height.

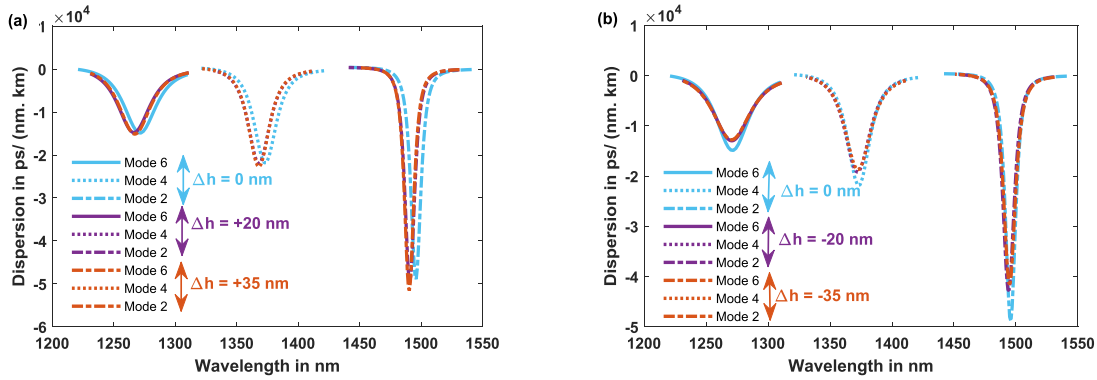

Fig. 9. Effect of (a) increase in rib height (b) decrease in rib height on dispersion profile of hybrid modes.

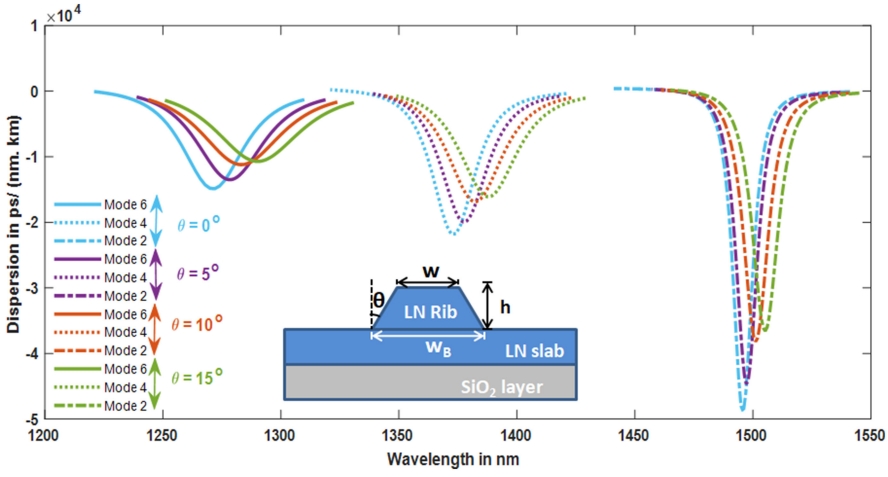

Fig. 10. Effect of angled side walls of LN rib on dispersion profile of hybrid modes.

Dispersion value can be further altered by designing a non-rectangular cross section of waveguides with angled sidewalls, which occur naturally during the fabrication process [22]. It was observed from simulation results that angled sidewalls have a significant effect on the resonant wavelengths as well as the dispersion peaks. Dispersion peaks red shift with the increase in the side wall angle as can be inferred from Fig. 10. It can also be inferred that the magnitude of peak dispersion changed by almost 25% for the three hybrid modes at a side wall angle of 15°. Another method to alter dispersion is by introducing bends in the waveguides [23].

The proposed multimode waveguide is a potential candidate for optically tunable true time delays (TTDs) in phased array antennas [24]. These can also serve as tunable dispersion compensators that enable adaptive compensation for dispersion fluctuations. Grating couplers can be designed to couple light from/to the fundamental mode in an optical fiber to/from the higher order mode in a multimode waveguide [25]. The dispersion peaks can be further broadened/tuned to achieve a larger FWHM, which could be useful in both telecom systems and optical signal processing for achieving multi-channel dispersion compensation.

4. Conclusion

In conclusion, we have theoretically illustrated large anomalous and normal dispersion (∼49000 ps/nm.km) for hybrid modes of a simple rib waveguide on LNOI. The three hybridization

regions in the waveguide allow large dispersion to be tuned at three distinct values. This multimode waveguide can also offer much lower dispersion when operated at a wavelength of 1550 nm (no hybrid modes). Dispersion is tunable over a wide range from ∼500 ps/(nm.km) to ∼50000 ps/(nm.km) by varying the wavelength from 1250 nm to 1550 nm. Proposed structure is relatively easy to fabricate compared to stacked waveguides and slot waveguides.

Acknowledgment

A. Kaushalram wishes to acknowledge the Visvesvaraya Ph.D. Scheme for Electronics and IT, Ministry of Electronics and Information Technology, Government of India, for financial assistance. The author would also like to thank Dr. N. Ramesh from SJC Institute of Technology, Yadunath T. R. from Applied Photonics Laboratory, and S. Aparanji from the Indian Institute of Science for fruitful discussions.

References

[1] H. Hu, R. Ricken, and W. Sohler, "Lithium niobate photonic wires," *Opt. Exp.*, vol. 17, no. 26, pp. 24261–24268, 2009. [Online]. Available: https://doi.org/10.1364/OE.17.024261

[2] G. Poberaj, H. Hu, W. Sohler, and P. Guenter, "Lithium niobate on insulator (LNOI) for micro-photonic devices," *Laser Photon. Rev.*, vol. 6, no. 4, pp. 488–503, 2012. [Online]. Available: https://doi.org/10.1002/lpor.201100035

[3] J. Schollhammer, M. A. Baghban, and K. Gallo, "Modal birefringence-free lithium niobate waveguides," *Opt. Lett.*, vol. 42, no. 18, pp. 3578–3581, 2017. [Online]. Available: https://doi.org/10.1364/OL.42.003578

[4] O. Stepanenko, E. Quillier, H. Tronche, P. Baldi, and M. de Micheli, "Highly confining proton exchanged waveguides on Z-Cut LiNbO3 with preserved nonlinear coefficient," *IEEE Photon.Technol. Lett.*, vol. 26, no. 15, pp. 1557–1560, Aug. 2014, doi: 10.1109/LPT.2014.2329134.

[5] S. S. Yohanes, S. S. Saha, M. Tsang, and A. J. Danner, "Rib microring resonators in lithium niobate on insulator," in *Proc. Int. Conf. Opt. MEMS Nanophoton.*, Jerusalem, Israel, 2015, pp. 1–2, doi: 10.1109/OMN.2015.7288825.

[6] C. E. Rüter, D. Kip, G. Stone, V. Dierolf, H. Hu, and W. Sohler, "Fluorescence in planar and ridge waveguides fabricated in Erbium-doped lithium-niobate-on-insulator (Er:LNOI)," in *Proc. Int. Conf. Lasers Electro-Opt. Eur. Int. Conf. Quantum Electron.*, Munich, Germany, 2013, pp. 1–1, doi: 10.1109/CLEOE-IQEC.2013.6801490.

[7] R. Wu *et al.*, "Long low-loss-litium niobate on insulator waveguides with sub-nanometer surface roughness," *Nanomaterials*, vol. 8, no. 11, 2018, Art. no. 910. [Online]. Available: https://doi.org/10.3390/nano8110910

[8] A. Kaushalram, G. Hegde, and S. Talabattula, "Comparative analysis of ultra-compact few-mode photonic wires on LNOI and SOI platforms," in *Proc. SPIE 10921, Integr. Opt., Devices, Mater., Technol. XXIII*, 2019, vol. 109211X, pp. 1–9. [Online]. Available: https://doi.org/10.1117/12.2508776

[9] L. Liu, Y. Ding, K. Yvind, and J. M. Hvam, "Efficient and compact TE–TM polarization converter built on silicon-on-insulator platform with a simple fabrication process," vol. 36, no. 7, pp. 1059–1061, 2011. [Online]. Available: https://doi.org/10.1364/OL.36.001059

[10] L. Cai, S. Zhang, and H. Hu, "A compact photonic crystal micro-cavity on a single-mode lithium niobate photonic wire," *J. Opt.*, vol. 18, no. 3, pp. 035801–035806, 2016. [Online]. Available: https://iopscience.iop.org/article/10.1088/2040-8978/18/3/035801/meta

[11] D. Dai, J. Wang, and S. He, "Silicon multimode photonic integrated devices for on-chip mode-division-multiplexed optical interconnects," *Prog. Electromagn. Res.*, vol. 143, pp. 773–819, 2013. [Online]. Available: http://www.jpier.org/PIER/pier.php?paper=13111003

[12] L. Zhang, Y. Yue, Y. Xiao-Li, R. G. Beausoleil, and A. E. Willner, "Highly dispersive slot waveguides," *Opt. Exp.*, vol. 17, no. 9, pp. 7095–7101, 2009. [Online]. Available: https://doi.org/10.1364/OE.17.007095

[13] M. R. Karim, B. M. A. Rahman, and G. P. Agarwal, "Mid-infrared supercontinuum generation using dispersion-engineered Ge11.5As24Se64.5 chalcogenide channel waveguide," *Opt. Exp.*, vol. 25, no. 5, pp. 6903–6914, 2015. [Online]. Available: https://doi.org/10.1364/OE.23.006903

[14] L. Zhang, M. Song, J.-Y. Yang, R. G. Beausoleil, and A. E. Willner, "A compact chromatic dispersion compensator using unequal and mutually-coupled microring resonators," in *Proc. Int. Conf. Integr. Photon. Nanophoton. Res. Appl.*, Boston, MA, USA, 2008, Paper IWA3. [Online]. Available: https://doi.org/10.1364/IPNRA.2008.IWA3

[15] D. T. H. Tan, K. Ikeda, R. E. Saperstein, B. Slutsky, and Y. Fainman, "Chip-scale dispersion engineering using chirped vertical gratings," *Opt. Lett.*, vol. 33, no. 24, pp. 3013–3015, 2008. [Online]. Available: https://doi.org/10.1364/OL.33.003013

[16] H. Tian, X. Zhang, D. Yang, and Y. Ji, "Research on the dispersion compensation of slot photonic crystal waveguide," *IEEE Photon. Technol. Lett.*, vol. 23, no. 17, pp. 1222–1224, Sep. 2011. [Online]. Available: https://doi.org/10.1109/LPT.2011.2158812

[17] N. Ashok, Y. L. Lee, and W. Shin, "Design and study of strip-slot waveguide structure for dispersion analysis," *IEEE Photon. J.*, vol. 8, no. 1, Feb. 2016, Art. no. 2700408. [Online]. Available: https://ieeexplore.ieee.org/document/7390156

[18] Y. Yue, L. Zhang, H. Huang, R. G. Beausoleil, and A. E. Willner, "Silicon-on-nitride waveguide with ultralow dispersion over an octave-spanning mid-infrared wavelength range," *IEEE Photon. J.*, vol. 4, no. 1, pp. 126–132, Feb. 2012, doi: 10.1109/JPHOT.2011.2180016.

[19] R. H. Khandokar, M. Bakaul, S. Skafidas, T. Nirmalathas, and M. Asaduzzaman, "Performance of planar, rib, and photonic crystal silicon waveguides in tailoring group-velocity dispersion and mode loss," *IEEE J. Sel. Topics Quantum Electron.*, vol. 22, no. 2, pp. 73–80, Mar./Apr. 2016, Art no. 4401308, doi: 10.1109/JSTQE.2015.2479359.
[20] [Online]. Available: https://www.lumerical.com
[21] D. E. Zelmon and D. L. Small, "Infrared corrected Sellmeier coefficients for congruently grown lithium niobate and 5 mol. % magnesium oxide–doped lithium niobate," *J. Opt. Soc. Amer. B*, vol. 14, no. 12, pp. 3319–3322, 1997. [Online]. Available: https://doi.org/10.1364/JOSAB.14.003319
[22] D. Dai and M. Zhang, "Mode hybridization and conversion in siliconon-insulator nanowires with angled sidewalls," *Opt. Exp.*, vol. 23, no. 25, pp. 32452–32464, 2015. [Online]. Available: https://doi.org/10.1364/OE.23.032452
[23] D. Dai, "Multimode optical waveguide enabling microbends with low inter-mode crosstalk for mode-multiplexed optical interconnects," *Opt. Exp.*, vol. 22, no. 22, pp. 27524–27534, 2014. [Online]. Available: https://doi.org/10.1364/OE.22.027524
[24] F. Scotti, P. Ghelfi, F. Laghezza, G. Serafino, S. Pinna, and A. Bogoni, "Flexible true-time-dealy beamforming in a photonics-based RF signals generator," in *Proc. 39th Eur. Conf. Opt. Commun.*, 2013, pp. 789–791, doi: 10.1049/cp.2013.1536.
[25] O. M. Nawwar, H. M. H. Shalaby, and R. K. Pokharel, "First-order mode compact focusing grating coupler for SOI interconnect," in *Proc. Int. Conf. IEEE Photon. Soc. Summer Top. Meet.*, Waikoloa Village, HI, USA, 2018, pp. 119–120, doi: 10.1109/PHOSST.2018.8456732.